

Fatigue Studies on Cryogenic Treated Dissimilar FSW AA6066-T6 and AA1060-T6 Aluminium Alloys

Nandakumar KOTHANDAM^{1*}, Lenin KASIRAJAN², Premraj YOGARAJ³,
Balamurugan SENTHAMARAIKANNAN⁴

¹ Department of Mechanical Engineering, M.A.M College of Engineering, Trichy, 621 105, Tamilnadu, India

² Department of Mechanical Engineering, K. Ramakrishnan College of Engineering, Trichy, 621 112, Tamilnadu, India

³ Department of Mechanical and Automation Engineering, Gojan School of Business and Technology, Chennai, 600 052, Tamilnadu, India

⁴ Department of Mechanical Engineering, Chennai Institute of Technology, Chennai, 600 069, Tamilnadu, India

<http://doi.org/10.5755/j02.ms.39775>

Received 11 December 2024; accepted 6 February 2025

The present research investigates the fatigue life of dissimilar friction stir welding (FSW) of AA6066-T6 and AA1060-T6 aluminium alloys that have undergone deep cryogenic treatment (DCT). The DCT-FSW alloy has fine, dense intermetallic phases, as evidenced by the microstructures of the welded zones of FSW. The uniaxial fatigue experiment was done to measure the number of cycles for failure and to plot the S-N curve. The fatigue fractures of both samples have been examined by SEM to investigate the fracture mode. Moreover, the fatigue life of the FSW and DCT-FSW joints was predicted using the Basquin method and the Acceleration Life Test (ALT). The predicted results revealed that the ALT method is more accurate than the Basquin method.

Keywords: friction stir welding, dissimilar aluminium alloys, deep cryogenic treatment, fatigue studies.

1. INTRODUCTION

Due to their outstanding strength-to-weight ratio, welded aluminium alloys are in great need in the automotive and aerospace industries [1–4]. The mechanical qualities of welded dissimilar aluminium alloys appear to be lost, and they are more susceptible to porosity and cracking. There have been problems using conventional fusion welding techniques [5–7]. One of the cheapest and greenest techniques to join similar and dissimilar aluminium alloys without adverse consequences like solidification and liquid cracking is friction stir welding (FSW) [8–10]. Dissimilar friction stir welding (FSW) has gained significant attention in modern manufacturing as an efficient technique for joining different materials while maintaining enhanced mechanical properties. The advancements in this domain are driven by innovative methodologies and an increasing emphasis on sustainable manufacturing practices [11–14]. A significant issue in design evaluation is structural fatigue. Therefore, researchers and designers are becoming increasingly interested in the fatigue properties of FSW jointed design. Enhancement of the friction process parameters was the objective of some earlier studies to improve fatigue properties [15–17]. FSW joints have better fatigue behaviour than TIG-welded joints in terms of quality [18]. Under welding process, it seems as though there are always potential faults, including root flaws, that are challenging to find with standard test methods. The main problem is a specific type of fault in FSW joints that exists

at the bottom side of the weld line and has a clear impact on how well the joints perform during fatigue [19, 20].

Vysotskiy et al. [21] discovered that the FSW heat-treated AA6061 had a higher fatigue strength than the parent material. The conventional heat treatment method is reinforced by the cryogenic treatment process, which improves the mechanical properties [22]. Liquid nitrogen is used in deep cryogenic treatment (DCT) to cool a substance to below 196°C. In order to enhance the mechanical and physical properties of materials, this treatment modifies their microstructure in a controlled, low-temperature environment [23–28]. The friction stir-welded Al-ZnCu alloy Al7050-T7451 joint's hardness, toughness, tensile strength, and elongation were all enhanced by cryogenic treatment [29]. In comparison to untreated samples, deep cryogenic treatment enhances the hardness and wear of the aluminium alloys 2024, 6082, and 7075 by 25 % [30]. In order to enhance the material qualities, the DCT has been explored and employed for years [31]. According to the literature review, very few studies focusing on the fatigue life of cryogenically treated dissimilar FSW welding were found. This study aims to investigate the impact of deep cryogenic treatment on the fatigue life of the FSW AA6066-AA1060 alloy, providing a comprehensive understanding of its performance characteristics. This research aims to investigate the fatigue life of the FSW AA6066-AA1060 aluminium alloy subjected to deep cryogenic treatment, with a particular focus on analysing the effects of rotation speed and weld speed on the alloy's microstructure and mechanical performance. Metallurgical studies are

* Corresponding author: K. Nandakumar
E-mail: nandakumar.mech@mamcet.com

conducted to examine the grain structure, intermetallic compounds (IMCs), and precipitates formed during FSW, with a comparison to those observed in DCT-FSW.

2. EXPERIMENTAL PROCEDURE

2.1. Materials

Manufactured alloy plates measuring $100 \times 75 \times 6$ mm and labelled AA6066-T6 and AA1060-T6 were used for dissimilar metal welding. The chemical composition of the purchased wrought alloys is given in Table 1. According to the author's previous work [32], the optimum parameter for welding AA1060 and AA6066 alloys was 1000 rpm tool rotation speed at 63 m/s welding speed. The optimum set of input parameters was used to prepare the FSW joints, as shown in Fig. 1.



Fig. 1 FSW processes for the alloys AA6066-T6 and AA1060-T6

2.2. Deep cryogenic treatment

Ten FSW joint samples with dimensions of $20 \times 15 \times 3$ mm in the transverse direction of the welded zone underwent DCT. Samples were submerged in a cryo can flask with liquid nitrogen at -196°C for deep cryogenic treatment. The samples were carefully removed from the flask after two hours [33, 34]. Following that, the samples were allowed to remain in the air for 30 minutes.

2.3. Microstructure studies

A few transversely bisected FSW and DCT welded joints were prepared and polished using different grades of silicon carbide paper, and then cloth polished with 3 mm and 1 mm diamond paste. Following polishing, the samples were etched using Keller's reagent (1 % HF, 1.5 % HCl, 2.5 % HNO₃, and 95 % distilled water). For the examination of microstructure, SEM was used.

2.4. Fatigue life test

Fatigue strength data are obtained at a stress ratio SR, of 0.1 with different maximum stresses of 132 to 75 MPa at a frequency of 10 Hz. The tests are carried out in the Instron fatigue testing machine as shown on Fig. 2 in laboratory air at ambient temperature. The standard flat specimens were prepared as per ASTM standard E 466.

Table 1. Chemical composition of alloys AA 6066 and AA 1060

Material	Mg	Zn	Mn	Ti	Cu	Fe	Si	Al
AA 6066, wt. %	0.82	0.25	0.6	0.01	0.7	0.01	0.9	96.71
AA 1060 wt. %	0.03	0.05	0.03	0.03	0.03	0.05	0.2	99.58

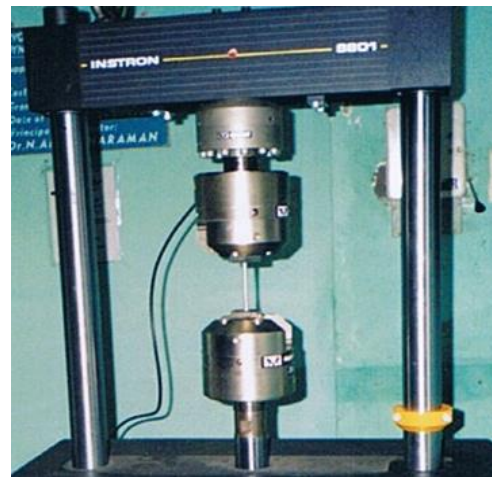


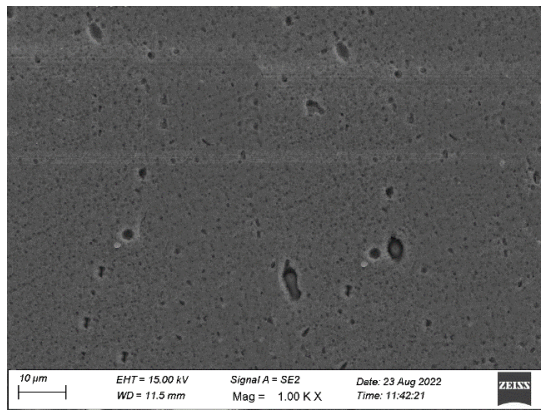
Fig. 2. Fatigue specimen loaded at Instron machine

3. RESULTS AND DISCUSSION

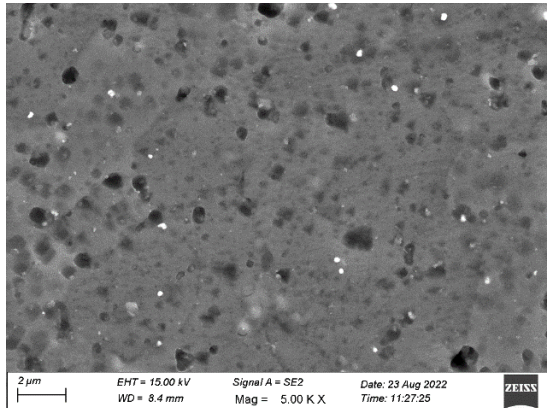
3.1. Microstructure

The macrographs and micrographs of the FSW and DCT-FSW joint weld zones are shown in Fig. 3. No flaws or cracks can be seen in Fig. 3 a. In the FSW-WZ zone microscopy, the stirring effect results in refined recrystallized grains with uniform grain size (Fig. 3 a and b). The increased magnification of Fig. 3 b depicts a fine Mg₂Al₃ precipitate phase scattered uniformly throughout the surface combined with needle-shaped Mg₂Si phases. High temperatures affect the FSW microstructure, significantly distort the spinning tool plastically, and activate dynamic recrystallization mechanisms [35]. The optimal tool rotation speed for FSW was 1000 rpm. This allowed for powerful mechanical contact over a wide area and material mixing in the welding zone (WZ). When the tool rotates quickly, the material is touched by the shoulder and pin. During the cryogenic treatment the dislocation motions are created, in which sub crystals are generated from the original grains, are what cause the grain refining. It is this dislocation impact that causes grain rotations and volume shrinkage. The material's properties are improved when the vacancies and micropores in the matrix compress [36].

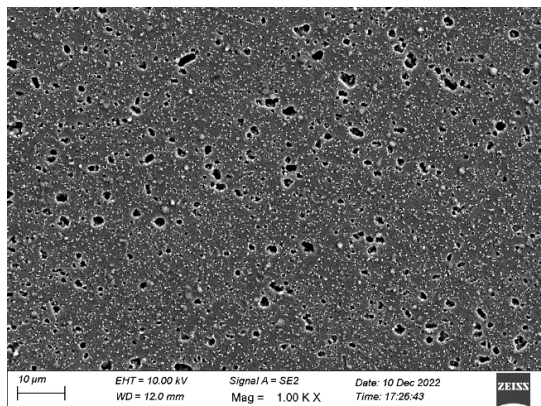
In DCT-WZ microstructure images (Fig. 3 c and d), the Mg₂Si phases are shown with a thick Mg₁₇Al₁₂ precipitate phase. Due to Mg's ability to reinforce the aluminium matrix and create new phases, the DCT of the FSW joint is improved. Sonar (2018) [37] recorded comparable outcomes. When comparing the micrographs in Fig. 3 a and b, the Mg₁₇Al₁₂ intermetallic generated marginally increases. Even with a small size increase, DCT recrystallizes coarse grains, increasing intermetallic volume.



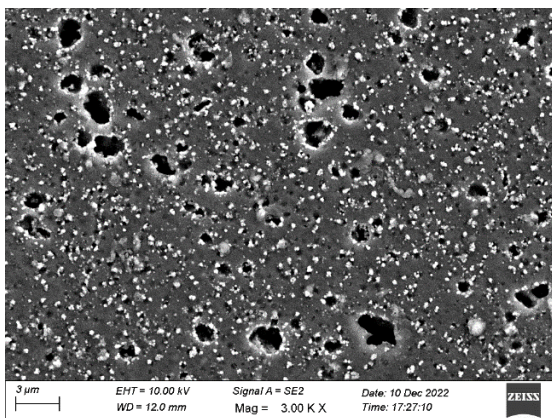
a



b



c



d

Fig. 3. SEM images: a, b—FSW joints: low and high magnification; c, d—DCT-FSW joints: low and high magnification

Because the intermetallic density is less than 2 %, X-ray diffraction cannot distinguish between the phases. The elements and intensities of the precipitate have been determined by SEM-EDX analysis and similar precipitate phases were reported by the same researchers in 2023 [38].

3.2. Fatigue life (S-N) curve

Fig. 4 presents the fatigue life experimental data through the S-N method for the samples of FSW and DCT-FSW joints. The maximum cycle has been attained at 75 MPa for the DCT-FSW sample, and the lowest cycle of 42932 has been obtained at 132 MPa for the FSW sample. In all stresses, DCT-FSW samples exhibited a higher fatigue life cycle than FSW samples. The image also shows that the curve with the highest slope has been generated by employing a maximum level of stress. The failure cycles for FSW and DCT-FSW are closer to each other at higher stress ranges. At a lower stress level, the failure cycle deviation is greater, which is elucidated in Fig. 4. The increase in fatigue strength of the DCT-FSW joint can be due to the formation of more intermetallic compounds.

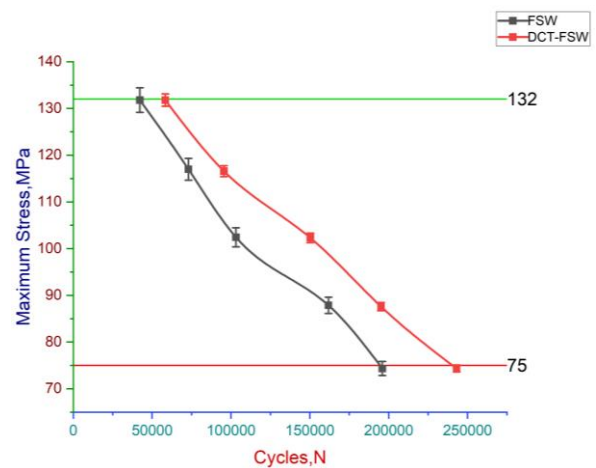
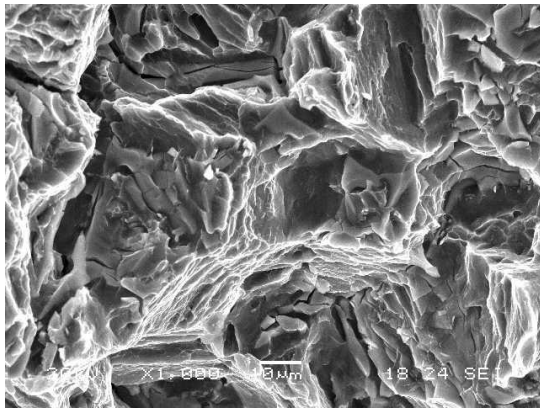


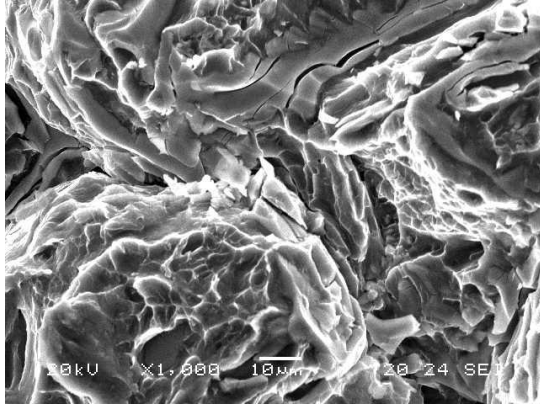
Fig. 4. S-N curve of FSW and DCT-FSW

Fig. 5 shows the SEM images of fatigue-fractured samples. Fig. 5 a represents minor cracks and dimples in the surface of the FSW sample fractured at 75 MPa stress further, at maximum stress of 132 MPa, secondary cracks and shallow dimples are seen in Fig. 5 b. Sonar et al. [39] identified ductile mode with dimples and brittle mode with striation in the fatigue fracture surface of the 1060 Al alloy. The plastic deformation has been seen in FSW samples, which makes it quasi-cleavage fracture mode. No cracks have been seen in Fig. 5 c and d moreover, dimples of small size seem to be present in the DCT-FSW fractured samples. The cryogenic treatment plays a significant role in shrinking the size of the dimples, and the intermetallic compound also improves the fatigue life. The greater the number of compound formations, the smaller the dimples on the surface. A similar observation has been reported by Li et al [40]. The fatigue striation has been observed in the DCT-FSW samples. The DCT-FSW sample shows a quasi-cleavage fracture mode.

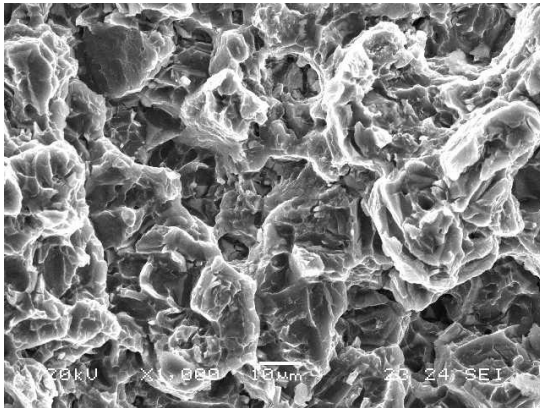
Fractography revealed the primary cracks that caused a fatigue failure that started on the specimens' free surface at both temperature conditions. The primary mechanism of deformation during cyclic loading was dislocation slip.



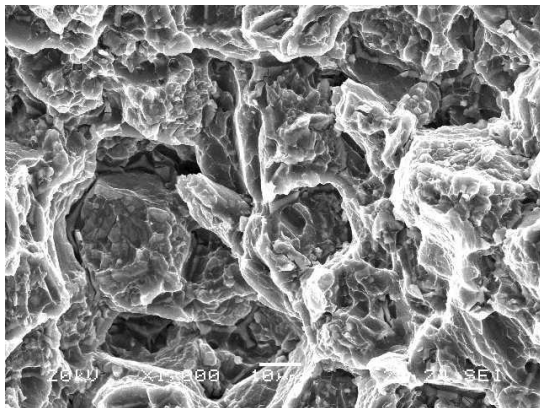
a



b



c



d

Fig. 5. SEM images of fractured surface of fatigue samples at: a–75 MPa of FSW; b–132 MPa of FSW; c–75 MPa of DCT-FSW; d–132 MPa of DCT-FSW

Fatigue striations developed along the path of crack growth. Dimple ductile mode was found in the middle of the fractured sample. A greater number of dislocations were produced at cryogenic temperature to accommodate the necessary strain during cyclic loading since dislocation mobility was constrained. Additionally, during cryogenic treatment, the grain size decreased, resulting in smaller dimples.

3.3. Fatigue life prediction model

The total quantity of variables that make out the relationship between two key factors, the stress level (σ) and the number of cycles to failure (N), has been considered when modelling an S-N curve [41]. These factors can be taken to be both dependent and independent factors, as well as being able to be expressed in a natural form by using logarithmic conversions.

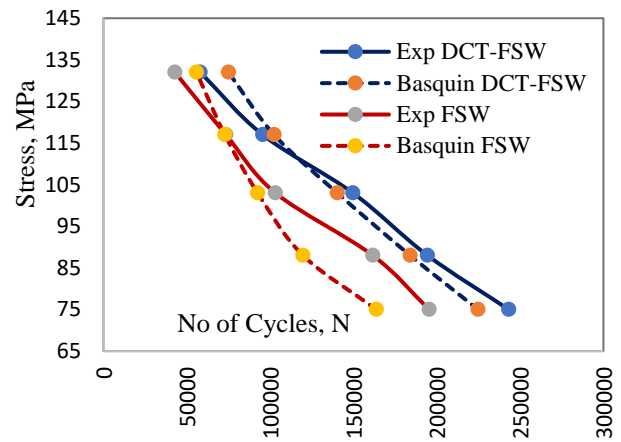


Fig. 6. Predicted (S-N) value by Basquin model

According to Basquin, fatigue resistance is inversely associated with the number of cycles essential to material failure, and it follows a power law. The S-N model developed by Basquin Eq. 1 [42]:

$$\sigma_m = \alpha (N_f)^a, \quad (1)$$

where σ_m stands for mean stress, α is for the coefficient of fatigue strength and a is for the exponent of fatigue strength. The predicted (S-N) values for the experimental data have been calculated using the Basquin equation, and the same is plotted as shown in Fig. 6. The graph inferred that predicted values were closer to the experimental data and intersected the experimental curve for both cases.

3.4. Accelerated life testing (ALT) for prediction of fatigue life

The illustration of a probability distribution is a focus of the Anderson-Darling (A-D) goodness-of-fit test method, which was calculated using MINITAB. Either the p-value or the A-D statistical value forms the basis for confirmation. Table 2 shows the A-D measurement calculates how well the results of the fatigue test conform to a specific distribution. It is a measurement of how far the real data points on a probability plot deviate from the fitted line. Higher weights are seen in the tails of the distribution and represent the weighted squared distance between the plot

points and the fitted line. A low A-D number often denotes a better fit between the provided distribution and the data.

Table 2. Anderson-Darling value of fatigue life

Stress, MPa	FSW	DCT-FSW
75	3.584	3.476
88	3.342	3.768
103	3.039	4.072
117	3.113	3.651
132	4.553	3.542

The results indicate that cryogenic treatment significantly influences the microstructure and mechanical properties of the dissimilar FSW joints, leading to enhanced fatigue resistance. Moreover, the fatigue life and failure modes are elucidated, highlighting the critical regions susceptible to fatigue damage. The novel approach presented in this study contributes to a comprehensive understanding of fatigue behavior in dissimilar FSW joints, offering valuable insights for optimizing welding processes and improving the structural integrity of welded components in cryogenic applications. Fatigue tests conducted under varying stress levels elucidate the fatigue life and failure mechanisms of the dissimilar FSW joints. Cryogenically treated specimens exhibit prolonged fatigue life compared to untreated counterparts, showcasing the beneficial effects of cryogenic treatment on fatigue resistance. Fractographic analysis of fatigue-tested specimens highlights the initiation and propagation of fatigue cracks, with a particular focus on critical regions such as the weld interface and heat-affected zone (HAZ). Cryogenic treatment mitigates crack initiation and retards crack propagation, contributing to improved fatigue performance.

The accelerated life testing (ALT) approach to reliability testing is more effective and less expensive. In order to gain knowledge on items with a long life well in advance, ALT seeks to hasten the failure process. The fatigue test data in accelerated settings is correlated with ALT. The results are extrapolated to conditions of typical use using this technique. Through acceleration testing, Weibull condition data can be predicted using accelerated life data. The probability sheet shows that the life data under accelerated conditions are parallel to one another, which supports the ALT programme. Failure rate graphs, as shown in Fig. 7 and Fig. 8, are particularly helpful since they show the system's failure pattern.

Table 3. ALT Predicted cycles and experimental cycles

Stress, MPa	FSW, no of cycles		DCT-FSW, no of cycles	
	Experimental	Predicted	Experimental	Predicted
75	195451	202809	243216	254523
88	161639	172398	194451	196899
103	103211	97601	149713	147997
117	73500	72924	95564	94205
132	42892	43884	58109	69481

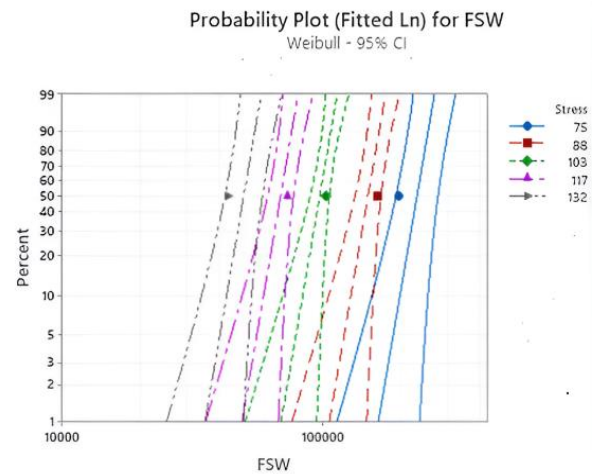


Fig. 7. Acceleration probability plot for FSW

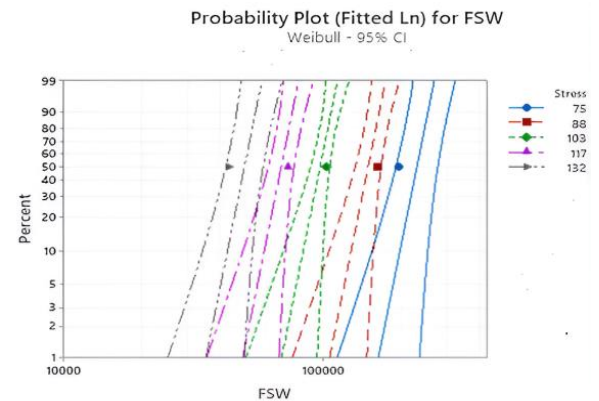


Fig. 8. Acceleration probability plot for DCT-FSW

Table 3 compares measured fatigue life data with an accelerated prediction of fatigue life. The results of the fatigue life prediction were more accurate. It is clear that the results of the measured values and the expected fatigue life are in good accord. As a result, this research offers a practical way to predict a particular target life in an area with limited lifespans and significant stresses. Future research should investigate the long-term behavior of cryogenically treated FSW alloys under conditions such as cyclic loading, corrosive environments, and high temperatures.

4. CONCLUSIONS

The findings of the fatigue life of the FSW AA6066-AA1060 alloy with and without DCT have been summarized as follows:

1. The refinement was caused by the needle-shaped Mg_2Si phases and the Mg_2Al_3 precipitate, according to the results observed under a microscope.

- DCT's impact causes dense Mg₁₇Al₁₂ to appear in the DCT-WZ, perhaps strengthening it over time.
- The coarse grain recrystallization of the WZ samples on SEM analysis resulted in a higher intermetallic density for the DCT-WZ samples. It is less common for the Mg₂Si phase to develop after cryogenic treatment. Aluminum near coarse grains experience significant plastic deformation because of the increased volume change and dislocation density brought on by DCT.
 - At higher stress ranges, the failure cycles for FSW and DCT-FSW become more similar, and at a maximum stress of 132 MPa, secondary cracks and shallow dimples were observed on the fractured surface of the FSW joint.
 - As a result of the increased compound growth, the dimples on the surface of the DCT-FSW joint are smaller.
 - The predicted (S-N) values for FSW and DCT-FSW were closer to the experimental data using the Basquin method, while the ALT method provided even greater accuracy.

REFERENCES

- Esfahani, Z., Rahimi, E., Sarvghad, M., Rafsanjani-Abbasi, A., Davoodi, A.** Correlation Between the Histogram and Power Spectral Density Analysis of AFM and SKPFM Images in an AA7023/AA5083 FSW Joint *Journal of Alloys and Compounds* 744 2018: pp. 174–181.
<https://doi.org/10.1016/j.jallcom.2018.02.106>
- Gullino, A., Matteis, P., D'Aiuto, F.** Review of Aluminum-to-Steel Welding Technologies for Car-Body Applications *Metals* 9 (3) 2019: pp. 315.
<https://doi.org/10.3390/met/9030315>
- Das, S.K., Gain, S., Sahoo, P.** Friction Stir Welding. In: Davim, J.P. (eds) *Welding Technology. Materials Forming, Machining and Tribology*. Springer, Cham. 2021: pp. 1–39.
https://doi.org/10.1007/978-3-030-63986-0_1
- Mastanaiah, P., Reddy, G.M., Sharma, A.** Evolution and Current Practices in Friction Stir Welding Tool Design *Advanced Welding and Deforming* 2021: pp. 151–177.
- Kasman, Ş., Yenier, Z.** Analyzing Dissimilar Friction Stir Welding of AA5754 / AA7075 *The International Journal of Advanced Manufacturing Technology* 70 2014: pp. 145–156.
<https://doi.org/10.1007/s00170-013-5256-7>
- Zhang, F., Su, X., Chen, Z., Nie, Z.** Effect of Welding Parameters on Microstructure and Mechanical Properties of Friction Stir Welded Joints of a Super High Strength Al–Zn–Mg–Cu Aluminum Alloy *Materials & Design* 67 2015: pp. 483–491.
<https://doi.org/10.1016/j.matdes.2014.10.055>
- Sajid, M., Kumar, G., Mehdi, H., Kumar, M.** Mechanical Characterization of FSWed Joints of Dissimilar Aluminum Alloys of AA7050 and AA6082 *Friction Stir Welding and Processing: Fundamentals to Advancements* 2024: pp. 125–133.
- Yogaraj, P., Kasirajan, L., Senthamaraiannan, B.** Effect of Tool Pin Positioning Factors on the Strength Behavior of Dissimilar Joints of AA5754-H111 and AA6101-T6 by Using Friction Stir Welding *Transaction of Indian Institute of Metals* 76 2023: pp. 3021–3030.
<https://doi.org/10.1007/s12666-023-03078-x>
- Shaik, B., Harinath Gowd, G., Durga Prasad, B.** Investigations and Optimization of Friction Stir Welding Process to Improve Microstructures of Aluminum Alloys *Cogent Engineering* 6 (1) 2019: pp. 1616373.
<https://doi.org/10.1080/23311916.2019.1616373>
- Balamurugan, S., Jayakumar, K., Nandakumar, C.** Investigation of Mechanical, Metallurgical and Corrosion Characteristics of Friction Stir Welded Dissimilar AA 5052-H32 and AA 6061-T6 Joints *Journal of the Chinese Institute of Engineers* 46 (6) 2023: pp. 601–614.
<https://doi.org/10.1080/02533839.2023.2227875>
- Astakhov, V.P.** Design of Experiment Methods in Manufacturing: Basics and Practical Applications. *In Statistical and computational techniques in manufacturing*. Berlin, Heidelberg: Springer Berlin Heidelberg. 2012: pp. 1–54.
<https://doi.org/10.1007/978-3-642-25859-6>
- Davim, J.P.** Sustainable and Intelligent Manufacturing: Perceptions in Line with 2030 Agenda of Sustainable Development *BioResources* 19 (1) 2024: pp. 4–5.
- Davim, J.P.** Perceptions of Industry 5.0: Sustainability Perspective *BioResources* 20 (1) 2025: pp. 15–16.
- Davim, J.P.** Manufacturing: A Bibliometric Analysis *International Journal of Manufacturing, Materials, and Mechanical Engineering (IJMMME)* 13 (1) 2024: pp. 1–4.
- Zhang, Z., Xiao, B.L., Ma, Z.Y.** Effect of Welding Parameters on Microstructure and Mechanical Properties of Friction Stir Welded 2219Al-T6 Joints *Journal of Materials Science* 47 2012: pp. 4075–4086.
<https://doi.org/10.1007/s10853-012-6261-1>
- Moghadam, D.G., Farhangdoost, K., Nejad, R.M.** Microstructure and Residual Stress Distributions Under the Influence of Welding Speed in Friction Stir Welded 2024 Aluminum Alloy *Metallurgical and Materials Transactions B* 47 (3) 2016: pp. 2048–2062.
<https://doi.org/10.1007/s11663-016-0611-3>
- Şefika, K., Ozan, S.** Effects of Overlapping Formed Via Pin Off Setting on Friction Stir Weldability of AA7075-T651 Aluminum Alloy *Journal of Mechanical Science and Technology* 33 (2) 2019: pp. 819–828.
<https://doi.org/10.1007/s12206-019-0138-z>
- Motrunich, S., Klochkov, I., Poklaytsky, A.** High Cycle Fatigue Behavior of Thin Sheet Joints of Aluminium-Lithium Alloys Under Constant and Variable Amplitude Loading *Welding in the World* 64 2020: pp. 1971–1979.
<https://doi.org/10.1007/s40194-020-00976-2>

19. **Di, S., Yang Luan, G., Jian, B.** Comparative Study on Fatigue Properties Between AA2024-T4 Friction Stir Welds and Base Materials *Materials Science and Engineering A* 435 2006: pp. 389–395. <https://doi.org/10.1016/j.msea.2006.07.009>
20. **Dickerson, T.L., Przydatek, J.** Fatigue of Friction Stir Welds in Aluminum Alloys that Contain Root Flaws *International Journal of Fatigue* 25 (12) 2003: pp. 1399–1409. [https://doi.org/10.1016/S0142-1123\(03\)00060-4](https://doi.org/10.1016/S0142-1123(03)00060-4)
21. **Lertora, E., Campanella, D., Pizzorni, M., Mandolino, C., Buffa, G., Fratini, L.** Comparative Evaluation of The Effect of the Substrate Thickness and Inherent Process Defects on the Static and Fatigue Performance of FSW and Adhesive-Bonded Overlap-Joints in an AA6016 Alloy *Journal of Manufacturing Processes* 64 2021: pp. 785–792. <https://doi.org/10.1016/j.jmapro.2021.01.04>
22. **Vysotskiy, I., Malopheyev, S., Rahimi, S., Mironov, S., Kaibyshev, R.** Unusual Fatigue Behavior of Friction Stir Welded Al-Mg-Si aAlloy *Materials Science and Engineering: A* 760 2019: pp. 277–286. <https://doi.org/10.1016/j.msea.06.005>
23. **Xu, X. Ren, X., Hou, H., Luo, X.** Effects of Cryogenic and Annealing Treatment on Microstructure and Properties of Friction Stir Welded TA15 Joints *Materials Science and Engineering: A* 804 2021: pp. 140750. <https://doi.org/10.1016/j.msea.2021.140750>
24. **Lulay, K.E., Khan, K., Chaaya, D.** The Effect of Cryogenic Treatments on 7075 Aluminum Alloy *Journal of Materials Engineering and Performance* 11 (5) 2002: pp. 479–480. <https://doi.org/10.1361/105994902770343683>
25. **Xie, C., Wu, X., Min, N., Shen, Y.** Carbon Segregation Behavior of High-Carbon High-Alloy Steel During Deep Cryogenic Treatment Using 3DAP *Acta Metall Sin* 51 (3) 2015: pp. 325–332. <https://doi.org/10.11900/0412.1961.2014.00430>
26. **Wang, J., Fu, R., Li, Y., Zhang, J.** Effects of Deep Cryogenic Treatment and Low-Temperature Aging on the Mechanical Properties of Friction-Stir-Welded Joints of 2024-T351 Aluminum Alloy *Materials Science and Engineering: A* 609 2014: pp. 147–153. <https://doi.org/10.1016/j.msea.2014.04.077>
27. **Wang, K., Tan, Z., Gu, K., Gao, B., Gao, G., Misra, R.D.K., Bai, B.** Effect of Deep Cryogenic Treatment on Structure-Property Relationship in an Ultrahigh Strength Mn-Si-Cr Bainite/Martensite Multiphase Rail Steel *Materials Science and Engineering: A* 684 2017: pp. 559–566. <https://doi.org/10.1016/j.msea.2016.12.100>
28. **Li, H., Tong, W., Cui, J., Zhang, H., Chen, L., Zuo, L.** The Influence of Deep Cryogenic Treatment on The Properties of High-Vanadium Alloy Steel *Materials Science and Engineering: A* 662 2016: pp. 356–362. <https://doi.org/10.1016/j.msea.2016.03.039>
29. **Bansal, A., Singla, A.K., Dwivedi, V., Goyal, D.K., Singla, J., Gupta, M.K., Krolczyk, G.M.** Influence of Cryogenic Treatment on Mechanical Performance of Friction Stir Al-Zn-Cu Alloy Weldments *Journal of Manufacturing Processes* 56 2020: pp. 43–53. <https://doi.org/10.1016/j.jmapro.2020.04.067>
30. **Padmini, B.V., Sampathkumaran, P., Seetharamu, S., Naveen, G.J., Niranjana, H.B.** Investigation on the Wear Behavior of Aluminium Alloys at Cryogenic Temperature and Subjected to Cryo-Treatment *Materials Science and Engineering* 502 (1) 2019: pp. 012191. <https://doi.org/1088/1757-899X/502/1/012191>
31. **Da Silva, T.C., Da Silva, E.P.** Cryogenic Treatment Effect on Cyclic Behavior of Ni54Ti46 Shape Memory Alloy *Shape Memory and Super Elasticity* 7 (3) 2021: pp. 421–437. <https://doi.org/10.1007/s40830-021-00338-x>
32. **Nandakumar, K., Lenin, K., Ajith Kumar, K.K.** Corrosion Behaviour of Cryogenic-Treated Dissimilar FSW Al Alloys *Transactions of the Indian Institute of Metals* 2023: pp. 1–11. <https://doi.org/10.1007/s12666-023-03047-4>
33. **Wei, L., Wang, D., Li, H., Xie, D., Ye, F., Song, R., Zheng, G., Wu, S.** Effects of Cryogenic Treatment on the Microstructure and Residual Stress of 7075 Aluminum Alloy *Metals* 8 2018: pp. 273. <https://doi.org/10.3390/met8040273>
34. **Zhang, J., Liu, Y., Zhou, J., Feng, Z., Wang, S.** Kinetic Study on The Corrosion Behavior of AM60 Magnesium Alloy with Different Nd Contents *Journal of Alloys and Compounds* 629 2015: pp. 290–296. <https://doi.org/10.1016/j.jallcom.2014.12.143>
35. **Viceré, A., Roventi, G., Paoletti, C., Cabibbo, M., Bellezze, T.** Corrosion Behavior of AA6012 Aluminum Alloy Processed by ECAP and Cryogenic Treatment *Metals* 9 (4) 2019: pp. 408. <https://doi.org/10.3390/met9040408>
36. **Chanthini, M.K., Govindaraju, M., Arul, S.** Effect of Cryogenic Treatment on Mechanical Properties of Aluminium Alloy AA2014 *Journal of the Institution of Engineers (India): Series D* 101 2020: pp. 265–270. <https://doi.org/10.1007/s40033-020-00237-y>
37. **Sonar, T., Lomte, S., Gogte, C.** Cryogenic Treatment of Metal—a Review *Materials Today: Proceedings* 5 (11) 2018: pp. 25219–25228. <https://doi.org/10.1016/j.matpr.2018.10.324>
38. **Yogaraj, P., Kasirajan, L.** Identifying the Optimal Process Parameter on AA1100 Friction Stir Welded Joints *Tehnički vjesnik* 29 (3) 2022: pp. 957–964. <https://doi.org/10.17559/TV-20210707150253>
39. **Hassanifard, S., Varvani-Farahani, A.** A Comparative Study on Fatigue Response of Aluminum Alloy Friction Stir Welded Joints at Various Post-Processing and Treatments *Journal of Manufacturing Material Process* 5 2021: pp. 93. <https://doi.org/10.3390/jmmp5030093>

40. **Li, J., Feng, A., Zhou, J., Chen, H., Sun, Y., Tian, X., Huang, Y., Huang, S.** Enhancement of Fatigue Properties of 2024-T351 Aluminum Alloy Processed by Cryogenic Laser Peening *Vacuum* 2019: pp. 41–45.
<https://doi.org/10.1016/j.vacuum.2019.02.030>. 2019
41. **Barbosa, J.F., Correia, J.A.F.O., Freire Junior, R.C.S., Zhu, S.P., De Jesus, A.M.P.** Probabilistic S-N Fields Based on Statistical Distributions Applied to Metallic and Composite Materials: State of the Art *Advances in Mechanical Engineering* 11 (8) 2019: pp. 1–22.
<https://doi.org/10.1177/1687814019870395>
42. **Burhan, I., Kim, H.S.** SN Curve Models for Composite Materials Characterisation: An Evaluative Review *Journal of Composites Science* 2 (3) 2018: pp. 38.
<https://doi.org/10.3390/jcs 2030038>



© Kothandam et al. 2025 Open Access This article is distributed under the terms of the Creative Commons Attribution 4.0 International License (<http://creativecommons.org/licenses/by/4.0/>), which permits unrestricted use, distribution, and reproduction in any medium, provided you give appropriate credit to the original author(s) and the source, provide a link to the Creative Commons license, and indicate if changes were made.